Science Advances
AAAS

advances.sciencemag.org/cgi/content/full/6/31/eabb0055/DC1

Supplementary Materials for

Life cycle energy use and environmental implications of high-performance perovskite tandem solar cells

Xueyu Tian, Samuel D. Stranks, Fengqi You*

*Corresponding author. Email: fengqi.you@cornell.edu

Published 31 July 2020, *Sci. Adv.* **6**, eabb0055 (2020)
DOI: 10.1126/sciadv.abb0055

This PDF file includes:

Supplementary Figures

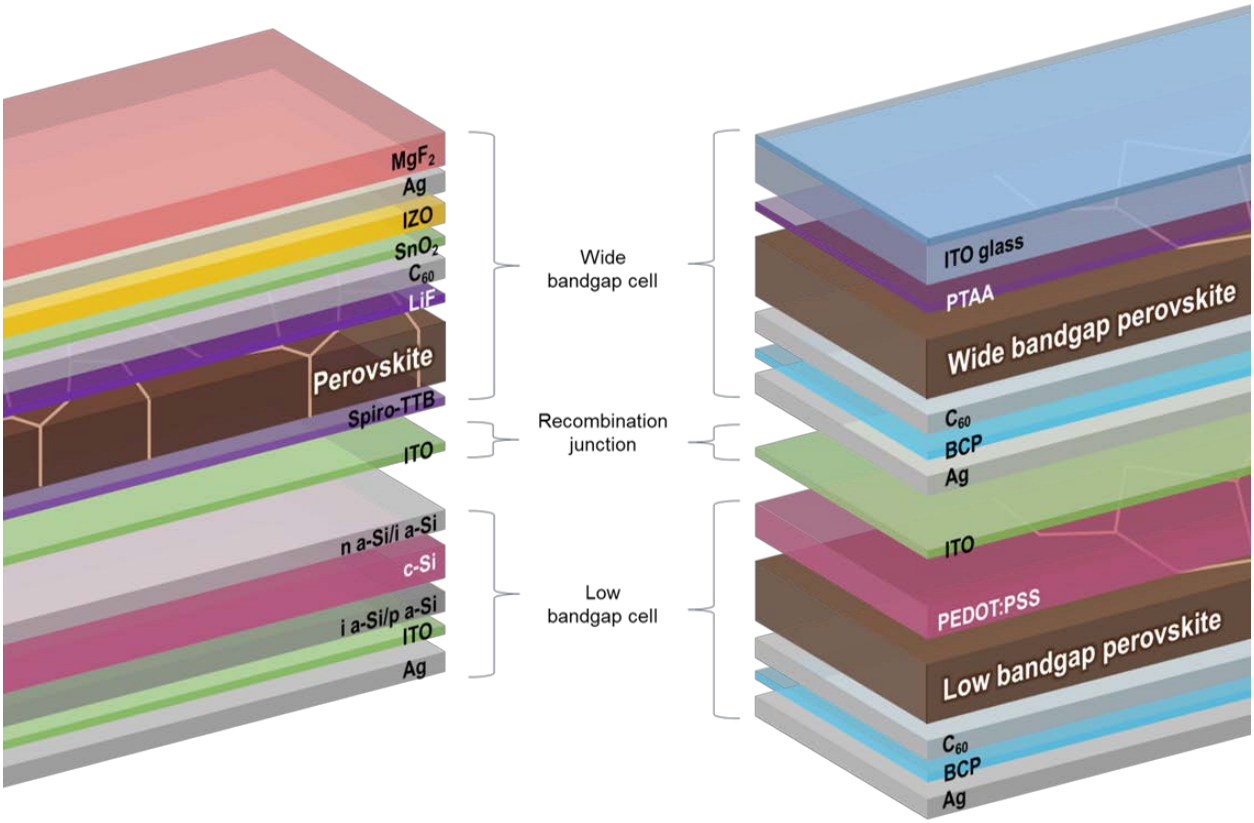

Fig. S1. Prototypical schematics of perovskite-silicon tandem solar cell (on the left) and perovskite-perovskite tandem solar cell (on the right) from the literature (*14, 17*).

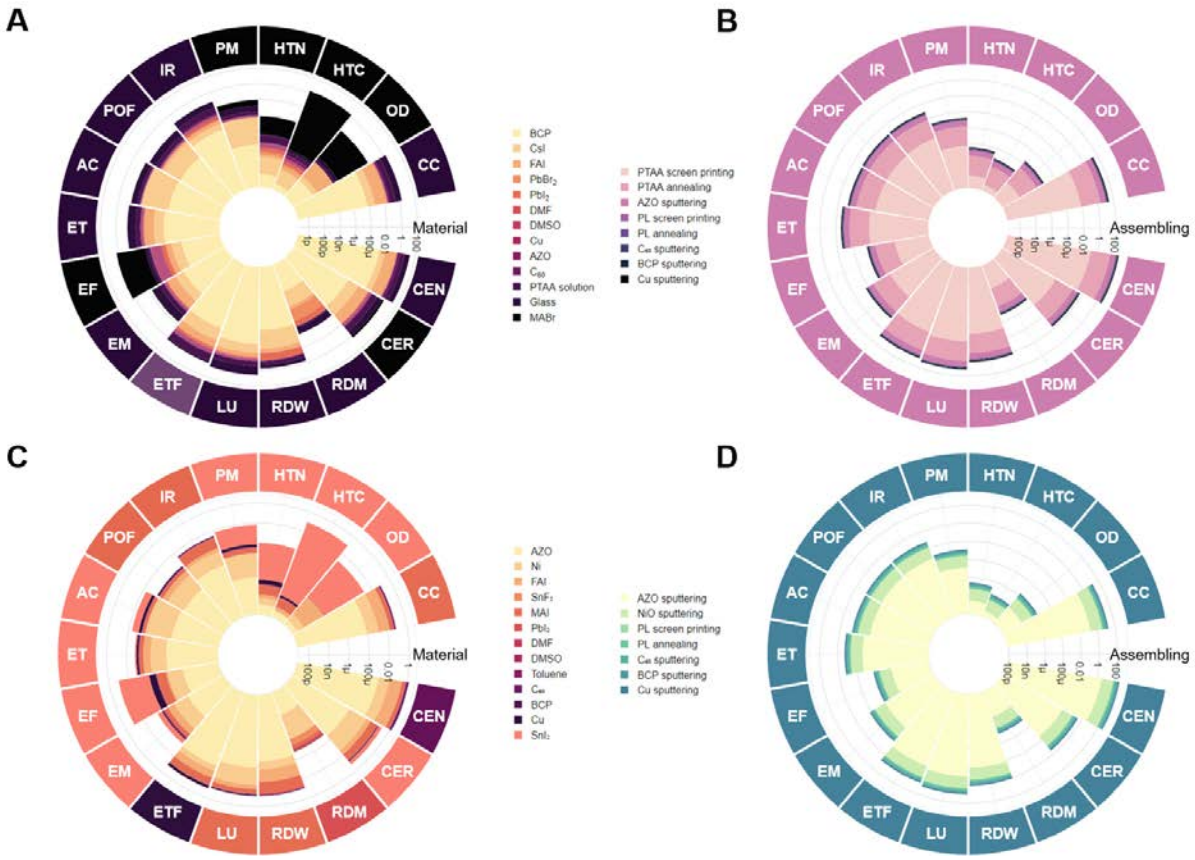

Fig. S2. Full-spectrum life cycle environmental impacts of a 1 m^2 of the perovskite-perovskite tandem solar cell on a logarithmic scale. Acronyms go counter clockwise: climate change (CC); ozone depletion (OD); human toxicity, cancer effects (HTC); human toxicity, non-cancer effects (HTN); particulate matter/respiratory effects (PM); ionizing radiation, human health (IR); photochemical ozone formation (POF); acidification (AC); eutrophication, terrestrial (ET); eutrophication, freshwater (EF); eutrophication, marine (EM); eco-toxicity, freshwater (ETF); land use (LU); resource depletion, water (RDW); resource depletion, mineral, fossil, renewable (RDM); cumulative energy demand, renewable (CER); cumulative energy demand, non-renewable (CEN). Life cycle environmental impacts embedded in the raw materials of the wide bandgap sub-cell (**A**). Life cycle environmental impacts associated with assembling phase of the wide bandgap sub-cell (**B**). Life cycle environmental impacts embedded in the raw materials of the low bandgap bottom cell (**C**). Life cycle environmental impacts associated with assembling phase of the low bandgap bottom cell (**D**).

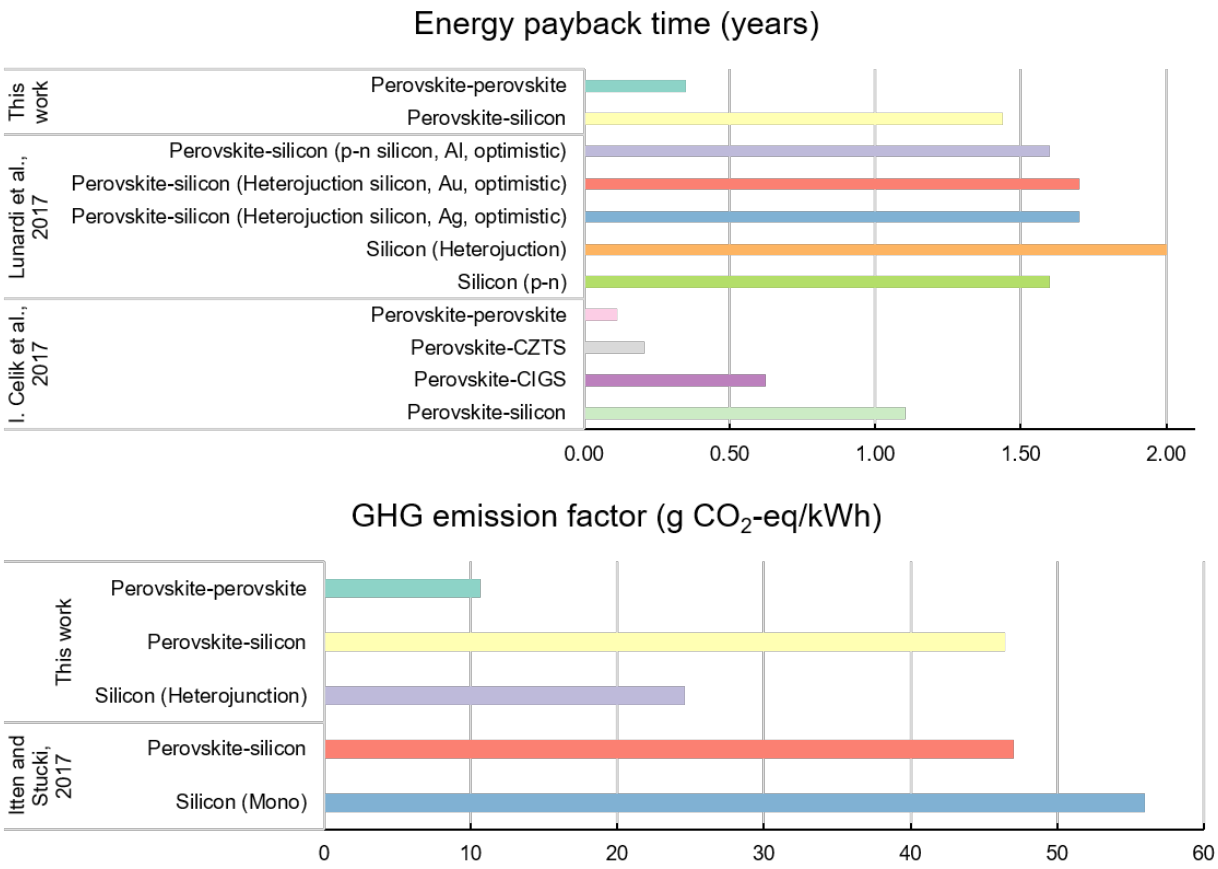

Fig. S3. Comparison of results regarding energy payback time and GHG emission factor in existing literature on tandem LCA (*8, 20, 23*).

Fig. S3 shows the results of EPBT and GHG emission factor reported in LCA studies on tandem perovskite PVs compared to the results obtained in this work. Referenced silicon PVs in each paper, if any, are also incorporated for a better understanding. In terms of EPBT, Lunardi et al. reported much higher values due to the use of energy-intensive spin-coating, expensive metals, and different grid conversion efficiency based on different assumption of electricity mix (*8*). Itten and Stucki reported higher GWP impacts than the values in this work, but the GHG emission factor of the perovskite-silicon tandem is close to that in this work because a longer lifetime of 30 years was assumed in their work (*23*).

Supplementary Tables

Table S1. Calibrated material inventory of 1 m^2 of the perovskite-silicon tandem solar cell and silicon heterojunction (SHJ) bottom cell (*17, 21*).

		Unit	Value
SHJ cell fabrication (*21*)			
Wafer production	Single-Si wafer	m^2	1.00E+00
Texturing/cleaning	Deionized water	kg	3.34E+01
	Hydrogen fluoride	kg	9.50E-02
	Sodium hydroxide	kg	1.56E-01
	Hydrogen peroxide	kg	5.60E-02
	Hydrochloride acid	kg	6.10E-02
	Ammonia	kg	1.10E-02
	Compressed air	m^3	2.50E-01
PECVD of a-Si:H	Deionized water	kg	3.94E+02
	Silane	kg	1.62E-03
	Hydrogen	kg	2.42E-03
	Oxygen	kg	2.60E-04
	NF_3 (for cleaning)	kg	2.20E-03
TCO sputtering	Deionized water	kg	5.12E+02
	ITO	kg	2.74E-03
Screen printing	Compressed air	m^3	1.10E+00
	Silver paste	kg	2.96E-02
Gas abatement	Deionized water	kg	1.20E+01
	Oxygen	kg	5.10E-03
	Nitrogen	kg	4.30E-03
	Propane	kg	3.30E-03
	Compressed air	m^3	1.40E-02
PSC fabrication			
	MgF_2	kg	2.47E-04
	Cu	kg	2.32E-04
	IZO	kg	8.65E-05
	SnO_2	kg	6.85E-05
	C_{60}	kg	2.48E-05
	LiF	kg	2.64E-06
	CsBr	kg	4.80E-05
	FAI	kg	1.55E-04
	PbI_2	kg	1.04E-03
	FABr	kg	1.41E-04
	Ethanol	kg	3.12E-03
	Spiro-TTB	kg	2.18E-05
	AZO	kg	9.27E-04
Encapsulation			
	Adhesive	kg	2.02E-02
	PET	kg	6.17E-02
Treatment	Fluid waste to treatment	m^3	3.35E-02
Direct emissions	Ethanol	kg	3.12E-03
Landfill		kg	1.04E+00

Table S2. Calibrated energy inventory of 1 m^2 of the perovskite-silicon tandem solar cell (*17*).

	Power (W)	Time (s)	Electricity (kWh)
SHJ cell fabrication (*21*)			
Texturing/cleaning	-	-	6.47E-01
PECVD of a-Si:H	-	-	6.59E+00
TCO sputter	-	-	6.30E+00
Screen printing	-	-	5.24E-01
Curing	-	-	3.10E-01
Gas abatement	-	-	4.50E-02
PSC fabrication			
MgF_2 sputtering	8.04E+04	182	4.10E+00
Cu sputtering	6.13E+04	218	3.74E+00
IZO sputtering	6.33E+04	200	3.53E+00
SnO_2 sputtering	6.80E+04	18	3.59E-01
C_{60} sputtering	6.63E+04	27	5.15E-01
LiF sputtering	6.04E+04	2	3.49E-02
Perovskite layer screen printing	6.42E+03	6	1.07E-02
Spiro-TTB screen printing	6.42E+03	6	1.07E-02
AZO sputtering	8.38E+04	91	2.15E+00
Encapsulation	1.50E+03	30	1.25E-02
Total			**28.88**

Table S3. Calibrated material inventory of 1 m^2 of the perovskite-perovskite tandem solar cell on glass (*14*).

	Unit	Value
Low bandgap PSC		
AZO	kg	9.27E-05
Ni	kg	9.06E-05
FAI	kg	2.05E-04
SnI_2	kg	4.43E-04
SnF_2	kg	1.87E-05
MAI	kg	1.26E-04
PbI_2	kg	3.66E-04
DMF	kg	9.36E-04
DMSO	kg	2.73E-04
Toluene	kg	6.88E-04
C_{60}	kg	3.96E-05
BCP	kg	5.62E-06
Cu	kg	7.17E-04
Wide bandgap PSC		
Solar glass	kg	1.54E+00
AZO	kg	3.71E-03
PTAA solution	kg	9.19E-03
CsI	kg	2.29E-05
FAI	kg	2.43E-04
MABr	kg	2.96E-05
$PbBr_2$	kg	9.71E-05
PbI_2	kg	6.91E-04
DMF	kg	8.88E-04
DMSO	kg	2.58E-04
C_{60}	kg	3.96E-05
BCP	kg	5.62E-06
Cu	kg	7.17E-04
Encapsulation		
Adhesive	kg	2.02E-02
PET	kg	6.17E-02
Direct emissions		
DMF	kg	1.82E-03
DMSO	kg	5.31E-04
Toluene	kg	1.99E-03
Acetonitrile	kg	7.86E-04
4-tert-butylpyridine	kg	6.92E-03
Landfill	kg	1.63E+00

Table S4. Calibrated energy inventory of 1 m^2 of the perovskite-perovskite tandem solar cell on glass (*14*).

	Power (W)	Time (s)	Electricity (kWh)
Low bandgap PSC fabrication			
AZO sputtering	8.38E+04	9	9.11E-01
NiO sputtering	9.83E+04	36	1.86E+01
Perovskite layer screen printing	6.42E+03	6	3.85E-02
Perovskite layer annealing	1.80E+04	600	1.08E+01
C_{60} sputtering	6.45E+04	55	1.85E+01
BCP sputtering	6.45E+04	11	1.57E+01
Cu sputtering	7.15E+04	182	2.80E+01
Wide bandgap PSC fabrication			
AZO sputtering	8.38E+04	364	4.55E+01
PTAA screen printing	6.42E+03	6	3.85E-02
PTAA annealing	1.80E+04	600	1.08E+01
Perovskite layer screen printing	6.42E+03	6	3.85E-02
Perovskite layer annealing	1.80E+04	600	1.08E+01
C_{60} sputtering	6.45E+04	55	1.85E+01
BCP sputtering	6.45E+04	11	1.57E+01
Cu sputtering	7.15E+04	182	2.80E+01
Encapsulation	1.50E+03	30	1.25E-02
Total			**61.65**

Table S5. LCI and LCIA results for 1 kg of C_{60} (*55*).

	Value	Unit
Process input		
O-xylene	2.400E+01	kg
Toluene	1.371E+02	kg
Oxygen	1.097E+02	kg
Electricity	2.233E+02	kWh
Process output		
C_{60}	1.000E+00	kg

Impact categories [Unit]	**Value**
Radiative forcing as Global Warming Potential (GWP100) [kg CO_2 eq.]	5.394E+02
Ozone Depletion Potential (ODP) [kg CFC-11 eq.]	2.258E-05
Comparative Toxic Unit for humans [CTUh, c]	3.012E-06
Comparative Toxic Unit for humans [CTUh, n-c]	1.332E-05
Intake fraction for fine particles [kg PM2.5 eq]	2.110E-01
Human exposure efficiency relative to U235 [kg U235 eq.]	1.267E+01
Tropospheric ozone concentration increase [kg NMVOC eq.]	1.471E+00
Accumulated Exceedance (AE) [mol H^+ eq.]	1.748E+00
Accumulated Exceedance (AE) [mol N eq.]	4.197E+00
Fraction of nutrients reaching freshwater end compartment (P)[kg P eq.]	5.803E-02
Fraction of nutrients reaching marine end compartment (N) [kg N eq.]	3.951E-01
Comparative Toxic Unit for ecosystems [CTUe]	1.536E+02
Soil Organic Matter [kg C deficit]	1.903E+02
Water abstraction related to local scarcity of water [m^3 water eq.]	3.722E+02
Scarcity [kg Sb eq.]	5.967E-04
Gross energy content of renewable primary energy resources [MJ eq.]	1.792E+02
Gross energy content of nonrenewable primary energy resources [MJ eq.]	1.470E+04

Table S6. LCI and LCIA results for 1 kg of tin chloride (*56*).

	Value	Unit
Process input		
Hydrochloric acid	4.140E-01	kg
Nitrogen	2.880E-01	kg
Tin	6.840E-01	kg
Steam	4.450E+00	kg
Electricity	7.917E-01	kWh
Deionized water	4.500E+00	kg
Cooling water	4.000E+02	kg
Process output		
Tin chloride	1.000E+00	kg
Wastewater	4.600E+00	kg
Hydrogen chloride	4.140E-04	kg

Impact categories [Unit]	**Value**
Radiative forcing as Global Warming Potential (GWP100) [kg CO_2 eq.]	1.021E+01
Ozone Depletion Potential (ODP) [kg CFC-11 eq.]	1.077E-06
Comparative Toxic Unit for humans [CTUh, c]	2.159E-07
Comparative Toxic Unit for humans [CTUh, n-c]	4.771E-06
Intake fraction for fine particles [kg PM2.5 eq]	3.082E-02
Human exposure efficiency relative to U235 [kg U235 eq.]	9.323E-01
Tropospheric ozone concentration increase [kg NMVOC eq.]	6.756E-02
Accumulated Exceedance (AE) [mol H^+ eq.]	1.035E-01
Accumulated Exceedance (AE) [mol N eq.]	2.996E-01
Fraction of nutrients reaching freshwater end compartment (P)[kg P eq.]	1.859E-02
Fraction of nutrients reaching marine end compartment (N) [kg N eq.]	2.345E-02
Comparative Toxic Unit for ecosystems [CTUe]	1.253E+01
Soil Organic Matter [kg C deficit]	2.529E+01
Water abstraction related to local scarcity of water [m^3 water eq.]	6.324E+00
Scarcity [kg Sb eq.]	1.305E-01
Gross energy content of renewable primary energy resources [MJ eq.]	1.202E+01
Gross energy content of nonrenewable primary energy resources [MJ eq.]	1.409E+02

Table S7. LCI and LCIA results for 1 kg of tin iodide (*56*).

	Value	Unit
Process input		
Iodine	7.400E-01	kg
Nitrogen gaseous	2.880E-01	kg
Tin chloride	5.510E-01	kg
Steam	4.450E+00	kg
Electricity	7.917E-01	kWh
Deionized water	4.500E+00	kg
Cooling water	4.000E+02	kg
Process output		
Tin iodide	1.000E+00	kg
Wastewater	4.790E+00	kg

Impact categories [Unit]	**Value**
Radiative forcing as Global Warming Potential (GWP100) [kg CO_2 eq.]	1.209E+01
Ozone Depletion Potential (ODP) [kg CFC-11 eq.]	3.420E+00
Comparative Toxic Unit for humans [CTUh, c]	2.125E+02
Comparative Toxic Unit for humans [CTUh, n-c]	2.513E-01
Intake fraction for fine particles [kg PM2.5 eq]	1.446E+01
Human exposure efficiency relative to U235 [kg U235 eq.]	2.852E-02
Tropospheric ozone concentration increase [kg NMVOC eq.]	3.102E-03
Accumulated Exceedance (AE) [mol H^+ eq.]	8.454E+00
Accumulated Exceedance (AE) [mol N eq.]	9.067E-01
Fraction of nutrients reaching freshwater end compartment (P)[kg P eq.]	2.400E+02
Fraction of nutrients reaching marine end compartment (N) [kg N eq.]	4.854E-01
Comparative Toxic Unit for ecosystems [CTUe]	1.648E+01
Soil Organic Matter [kg C deficit]	5.067E+00
Water abstraction related to local scarcity of water [m^3 water eq.]	1.548E-01
Scarcity [kg Sb eq.]	5.711E-03
Gross energy content of renewable primary energy resources [MJ eq.]	2.264E+02
Gross energy content of nonrenewable primary energy resources [MJ eq.]	1.212E+00

Table S8. LCI and LCIA results for 1 kg of caesium bromide (*56*).

	Value	Unit
Process input		
Cs_2CO_3	8.320E-01	kg
Hydrobromic acid	4.130E-01	kg
Nitrogen gaseous	2.880E-01	kg
Steam	4.450E+00	kg
Electricity	7.917E-01	kWh
Deionized water	4.500E+00	kg
Cooling water	4.000E+02	kg
Process output		
Caesium bromide	1.000E+00	kg
Wastewater	4.750E+00	kg

Impact categories [Unit]	**Value**
Radiative forcing as Global Warming Potential (GWP100) [kg CO_2 eq.]	7.812E+00
Ozone Depletion Potential (ODP) [kg CFC-11 eq.]	1.053E-06
Comparative Toxic Unit for humans [CTUh, c]	1.380E-07
Comparative Toxic Unit for humans [CTUh, n-c]	1.306E-06
Intake fraction for fine particles [kg PM2.5 eq]	5.166E-03
Human exposure efficiency relative to U235 [kg U235 eq.]	3.397E-01
Tropospheric ozone concentration increase [kg NMVOC eq.]	2.087E-02
Accumulated Exceedance (AE) [mol H^+ eq.]	4.127E-02
Accumulated Exceedance (AE) [mol N eq.]	8.821E-02
Fraction of nutrients reaching freshwater end compartment (P)[kg P eq.]	2.736E-03
Fraction of nutrients reaching marine end compartment (N) [kg N eq.]	1.166E-02
Comparative Toxic Unit for ecosystems [CTUe]	5.511E+00
Soil Organic Matter [kg C deficit]	1.935E+01
Water abstraction related to local scarcity of water [m^3 water eq.]	1.132E+01
Scarcity [kg Sb eq.]	3.341E-03
Gross energy content of renewable primary energy resources [MJ eq.]	3.933E+00
Gross energy content of nonrenewable primary energy resources [MJ eq.]	1.057E+02

Table S9. LCI and LCIA results for 1 kg of caesium iodide (*57*).

	Value	Unit
Process input		
Sulfuric acid	7.550E-01	kg
Lime	4.317E-01	kg
Iodine	4.884E-01	kg
Hydrogen	3.849E-03	kg
Deionized water	1.027E+01	kg
Pollucite ore	1.695E+00	kg
Crushing	1.695E+00	kg
Heat	1.289E+01	MJ
Electricity	2.700E-02	kWh
Process output		
Water (emission to air)	9.925E+00	kg
Aluminium oxide (emission to water)	1.962E-01	kg
Silicon dioxide (emission to water)	9.250E-01	kg
Sodium hydroxide (emission to water)	3.040E-01	kg
Waste gypsum	1.332E+03	kg
Caesium iodide	1.000E+00	kg

Impact categories [Unit]	**Value**
Radiative forcing as Global Warming Potential (GWP100) [kg CO_2 eq.]	2.326E+01
Ozone Depletion Potential (ODP) [kg CFC-11 eq.]	5.110E-06
Comparative Toxic Unit for humans [CTUh, c]	1.128E-06
Comparative Toxic Unit for humans [CTUh, n-c]	1.721E-05
Intake fraction for fine particles [kg PM2.5 eq]	2.017E+00
Human exposure efficiency relative to U235 [kg U235 eq.]	1.992E+00
Tropospheric ozone concentration increase [kg NMVOC eq.]	2.804E+00
Accumulated Exceedance (AE) [mol H^+ eq.]	4.294E+01
Accumulated Exceedance (AE) [mol N eq.]	5.372E-01
Fraction of nutrients reaching freshwater end compartment (P)[kg P eq.]	4.614E-03
Fraction of nutrients reaching marine end compartment (N) [kg N eq.]	4.962E-02
Comparative Toxic Unit for ecosystems [CTUe]	5.312E+01
Soil Organic Matter [kg C deficit]	2.230E+02
Water abstraction related to local scarcity of water [m^3 water eq.]	7.431E+01
Scarcity [kg Sb eq.]	1.328E-03
Gross energy content of renewable primary energy resources [MJ eq.]	1.214E+01
Gross energy content of nonrenewable primary energy resources [MJ eq.]	4.643E+02

REFERENCES AND NOTES

1. NREL, *Photovoltaic Research: Perovskite Solar Cells* (NREL, 2019); https://nrel.gov/pv/perovskite-solar-cells.html.
2. NREL, *NREL Transforming Energy: Best Research-Cell Efficiency Chart* (NREL, 2019); https://nrel.gov/pv/cell-efficiency.html.
3. C. Philibert, *Technology Roadmap: Solar Photovoltaic Energy* (International Energy Agency, 2014).
4. D. P. McMeekin, S. Mahesh, N. K. Noel, M. T. Klug, J. Lim, J. H. Warby, J. M. Ball, L. M. Herz, M. B. Johnston, H. J. Snaith, Solution-processed all-perovskite multi-junction solar cells. *Joule* **3**, 387–401 (2019).
5. M. T. Hörantner, T. Leijtens, M. E. Ziffer, G. E. Eperon, M. G. Christoforo, M. D. McGehee, H. J. Snaith, The potential of multijunction perovskite solar cells. *ACS Energy Lett.* **2**, 2506–2513 (2017).
6. F. Lang, M. Jošt, K. Frohna, A. A. Ashouri, A. R. Bowman, T. Bertram, A. B. Morales-Vilches, E. M. Tennyson, K. Galkowski, B. Stannowski, C. A. Kaufmann, R. Schlatmann, J. Bundesmann, A. Denker, J. Rappich, S. Albrecht, H.-C. Neitzert, N. H. Nickel, S. D. Stranks, Radiation hardness of perovskite/silicon and perovskite/CIGS tandem solar cells under proton irradiation, in *Proceedings of nanoGe Fall Meeting19 (NFM19)*, Berlin, Germany, 3 to 8 November 2019.
7. A. F. Palmstrom, G. E. Eperon, T. Leijtens, R. Prasanna, S. N. Habisreutinger, W. Nemeth, E. A. Gaulding, S. P. Dunfield, M. Reese, S. Nanayakkara, T. Moot, J. Werner, J. Liu, B. To, S. T. Christensen, M. D. McGehee, M. F. A. M. van Hest, J. M. Luther, J. J. Berry, D. T. Moore, Enabling flexible all-perovskite tandem solar cells. *Joule* **3**, 2193–2204 (2019).
8. M. Monteiro Lunardi, A. W. Y. Ho-Baillie, J. P. Alvarez-Gaitan, S. Moore, R. Corkish, A life cycle assessment of perovskite/silicon tandem solar cells. *Prog. Photovolt.* **25**, 679–695 (2017).
9. D. Zhao, C. Chen, C. Wang, M. M. Junda, Z. Song, C. R. Grice, Y. Yu, C. Li, B. Subedi, N. J. Podraza, X. Zhao, G. Fang, R.-G. Xiong, K. Zhu, Y. Yan, Efficient two-terminal all-perovskite tandem solar cells enabled by high-quality low-bandgap absorber layers. *Nat. Energy* **3**, 1093–1100 (2018).

10. H. Shen, T. Duong, J. Peng, D. Jacobs, N. Wu, J. Gong, Y. Wu, S. K. Karuturi, X. Fu, K. Weber, X. Xiao, T. P. White, K. Catchpolea, Mechanically-stacked perovskite/CIGS tandem solar cells with efficiency of 23.9% and reduced oxygen sensitivity. *Energy Environ. Sci.* **11**, 394–406 (2018).
11. M. Langenhorst, B. Sautter, R. Schmager, J. Lehr, E. Ahlswede, M. Powalla, U. Lemmer, B. S. Richards, U. W. Paetzold, Energy yield of all thin-film perovskite/CIGS tandem solar modules. *Prog. Photovolt.* **27**, 290–298 (2019).
12. Z. Li, Y. Zhao, X. Wang, Y. Sun, Z. Zhao, Y. Li, H. Zhou, Q. Chen, Cost analysis of perovskite tandem photovoltaics. *Joule* **2**, 1559–1572 (2018).
13. S. Albrecht, B. Rech, Perovskite solar cells: On top of commercial photovoltaics. *Nat. Energy* **2**, 16196 (2017).
14. J. Tong, Z. Song, D. H. Kim, X. Chen, C. Chen, A. F. Palmstrom, P. F. Ndione, M. O. Reese, S. P. Dunfield, O. G. Reid, J. Liu, F. Zhang, S. P. Harvey, Z. Li, S. T. Christensen, G. Teeter, D. Zhao, M. M. Al-Jassim, M. F. A. M. van Hest, M. C. Beard, S. E. Shaheen, J. J. Berry, Y. Yan, K. Zhu, Carrier lifetimes of >1 μs in Sn-Pb perovskites enable efficient all-perovskite tandem solar cells. *Science* **364**, 475–479 (2019).
15. G. E. Eperon, T. Leijtens, K. A. Bush, R. Prasanna, T. Green, J. T.W. Wang, D. P. McMeekin, G. Volonakis, R. L. Milot, R. May, A. Palmstrom, D. J. Slotcavage, R. A. Belisle, J. B. Patel, E. S. Parrott, R. J. Sutton, W. Ma, F. Moghadam, B. Conings, A. Babayigit, H.-G. Boyen, S. Bent, F. Giustino, L. M. Herz, M. B. Johnston, M. D. McGehee, H. J. Snaith, Perovskite-perovskite tandem photovoltaics with optimized band gaps. *Science* **354**, 861–865 (2016).
16. G. E. Eperon, M. T. Hörantner, H. J. Snaith, Metal halide perovskite tandem and multiple-junction photovoltaics. *Nat. Rev. Chem.* **1**, 0095 (2017).
17. F. Sahli, J. Werner, B. A. Kamino, M. Bräuninger, R. Monnard, B. Paviet-Salomon, L. Barraud, L. Ding, Juan J. Diaz Leon, D. Sacchetto, G. Cattaneo, M. Despeisse, M. Boccard, S. Nicolay, Q. Jeangros, B. Niesen, C. Ballif, Fully textured monolithic perovskite/silicon tandem solar cells with 25.2% power conversion efficiency. *Nat. Mater.* **17**, 820–826 (2018).
18. J. Werner, C.-H. Weng, A. Walter, L. Fesquet, J. P. Seif, S. De Wolf, B. Niesen, C. Balli, Efficient monolithic perovskite/silicon tandem solar cell with cell area >1 cm^2. *J. Phys. Chem. Lett.* **7**, 161–166 (2016).

19. J. Werner, B. Niesen, C. Ballif, Perovskite/silicon tandem solar cells: Marriage of convenience or true love story?—An overview. *Adv. Mater. Interfaces* **5**, 1700731 (2018).
20. I. Celik, A. B. Phillips, Z. Song, Y. Yan, R. J. Ellingson, M. J. Heben, D. Apul, Environmental analysis of perovskites and other relevant solar cell technologies in a tandem configuration. *Energ. Environ. Sci.* **10**, 1874–1884 (2017).
21. A. Louwen, W. G. J. van Sark, R. E. I. Schropp, W. C. Turkenburg, A. P. C. Faaij, Life-cycle greenhouse gas emissions and energy payback time of current and prospective silicon heterojunction solar cell designs. *Prog. Photovolt.* **23**, 1406–1428 (2015).
22. I. Celik, A. B. Philips, Z. Song, Y. Yan, R. J. Ellingson, M. J. Heben, D. Apul, Energy payback time (EPBT) and energy return on energy invested (EROI) of perovskite tandem photovoltaic solar cells. *IEEE J. Photovolt.* **8**, 305–309 (2018).
23. R. Itten, M. Stucki, Highly efficient 3rd generation multi-junction solar cells using silicon heterojunction and perovskite tandem: Prospective life cycle environmental impacts. *Energies* **10**, 841 (2017).
24. R. Frischknecht, G. Heath, M. Raugei, P. Sinha, M. de Wild-Scholten, *Methodology Guidelines on Life Cycle Assessment of Photovoltaic Electricity* (National Renewable Energy Laboratory, 2016).
25. L. Wang, G.-R. Li, Q. Zhao, X.-P. Gao, Non-precious transition metals as counter electrode of perovskite solar cells. *Energy Storage Mater.* **7**, 40–47 (2017).
26. J. Trube, *International Technology Roadmap for Photovoltaic (ITRPV)* (VDMA Photovoltaic Equipement, 2018).
27. Z. Liu, J. Chang, Z. Lin, L. Zhou, Z. Yang, D. Chen, C. Zhang, S. F. Liu, Y. Hao, High-performance planar perovskite solar cells using low temperature, solution–combustion-based nickel oxide hole transporting layer with efficiency exceeding 20%. *Adv. Energy Mater.* **8**, 1703432 (2018).
28. Q. Jiang, Z. Chu, P. Wang, X. Yang, H. Liu, Y. Wang, Z. Yin, J. Wu, X. Zhang, J. You, Planar-structure perovskite solar cells with efficiency beyond 21%. *Adv. Mater.* **29**, 1703852 (2017).
29. K. X. Steirer, J. P. Chesin, N. E. Widjonarko, J. J. Berry, A. Miedaner, D. S. Ginley, D. C. Olson, Solution deposited NiO thin-films as hole transport layers in organic photovoltaics. *Organic Electron.* **11**, 1414–1418 (2010).

30. J. You, C.-C. Chen, L. Dou, S. Murase, H.-S. Duan, S. A. Hawks, T. Xu, H. J. Son, L. Yu, G. Li, Y. Yang, Metal oxide nanoparticles as an electron-transport layer in high-performance and stable inverted polymer solar cells. *Adv. Mater.* **24**, 5267–5272 (2012).
31. Z. Li, T. R. Klein, D. H. Kim, M. Yang, J. J. Berry, M. F. A. M. van Hest, K. Zhu, Scalable fabrication of perovskite solar cells. *Nat. Rev. Mater.* **3**, 18017 (2018).
32. J. B. Whitaker, D. H. Kim, B. W. Larson, F. Zhang, J. J. Berry, M. F. A. M. van Hest, K. Zhu, Scalable slot-die coating of high performance perovskite solar cells. *Sustainable Energy Fuels* **2**, 2442–2449 (2018).
33. J. Jean, M. Woodhouse, V. Bulović, Accelerating photovoltaic market entry with module replacement. *Joule* **3**, 2824–2841 (2019).
34. B. J. Kim, D. H. Kim, S. L. Kwon, S. Y. Park, Z. Li, K. Zhu, H. S. Jung, Selective dissolution of halide perovskites as a step towards recycling solar cells. *Nat. Commun.* **7**, 11735 (2016).
35. Ecoinvent version 3.6 (Ecoinvent Centre, 2019); https://ecoinvent.org/.
36. J. Gong, S. B. Darling, F. You, Perovskite photovoltaics: Life-cycle assessment of energy and environmental impacts. *Energ. Environ. Sci.* **8**, 1953–1968 (2015).
37. N. Espinosa, R. García-Valverde, F. C. Krebs, Life-cycle analysis of product integrated polymer solar cells. *Energ. Environ. Sci.* **4**, 1547–1557 (2011).
38. M. M. de Wild-Scholten, Energy payback time and carbon footprint of commercial photovoltaic systems. *Solar Energy Mater. Solar Cells* **119**, 296–305 (2013).
39. N. Espinosa, M. Hösel, D. Angmo, F. C. Krebs, Solar cells with one-day energy payback for the factories of the future. *Energ. Environ. Sci.* **5**, 5117–5132 (2012).
40. E. A. Alsema, E. Nieuwlaar, Energy viability of photovoltaic systems. *Energy Policy* **28**, 999–1010 (2000).
41. V. M. Fthenakis, H. C. Kim, E. Alsema, Emissions from photovoltaic life cycles. *Environ. Sci. Technol.* **42**, 2168–2174 (2008).
42. M. A. Huijbregts, L. J. A. Rombouts, S. Hellweg, R. Frischknecht, A Jan Hendriks, D. Van de Meent, A. M. J. Ragas, L. Reijnders, J. Struijs, Is cumulative fossil energy demand a useful indicator for the environmental performance of products? *Environ. Sci. Technol.* **40**, 641–648 (2006).

43. N. Stylos, C. Koroneos, Carbon footprint of polycrystalline photovoltaic systems. *J. Clean. Prod.* **64**, 639–645 (2014).
44. N. Jungbluth, Life cycle assessment of crystalline photovoltaics in the Swiss ecoinvent database. *Prog. Photovolt.* **13**, 429–446 (2005).
45. V. M. Fthenakis, H. C. Kim, Photovoltaics: Life-cycle analyses. *Solar Energy* **85**, 1609–1628 (2011).
46. D. Yue, P. Khatav, F. You, S. B. Darling, Deciphering the uncertainties in life cycle energy and environmental analysis of organic photovoltaics. *Energ. Environ. Sci.* **5**, 9163–9172 (2012).
47. S. B. Darling, F. You, T. Veselka, A. Velosa, Assumptions and the levelized cost of energy for photovoltaics. *Energ. Environ. Sci.* **4**, 3133–3139 (2011).
48. D. Weltman, Using Monte Carlo simulation with Oracle© Crystal Ball to teach business students sampling distribution concepts. *Bus. Educ. Innov. J.* **7**, 59–63 (2015).
49. K. Treyer, C. Bauer, Life cycle inventories of electricity generation and power supply in version 3 of the ecoinvent database—Part I: Electricity generation. *Int. J. Life Cycle Assess.* **21**, 1236–1254 (2016).
50. R. Frischknecht, LCI modelling approaches applied on recycling of materials in view of environmental sustainability, risk perception and eco-efficiency. *Int. J. Life Cycle Assess.* **15**, 666–671 (2010).
51. N. Espinosa, L. Serrano-Luján, A. Urbina, F. C. Krebs, Solution and vapour deposited lead perovskite solar cells: Ecotoxicity from a life cycle assessment perspective. *Solar Energy Mater. Solar Cells* **137**, 303–310 (2015).
52. T. Stocker, D. Qin, G.-K. Plattner, M. Tignor, S.K. Allen, J. Boschung, A. Nauels, Y. Xia, V. Bex, P.M. Midgley, *IPCC, 2013: Climate Change 2013: The Physical Science Basis. Contribution of Working Group I to the Fifth Assessment Report of the Intergovernmental Panel on Climate Change* (Intergovernmental Panel on Climate Change, 2013).
53. K. P. Bhandari, J. M. Collier, R. J. Ellingson, D. S. Apul, Energy payback time (EPBT) and energy return on energy invested (EROI) of solar photovoltaic systems: A systematic review and meta-analysis. *Renew. Sustain. Energy Rev.* **47**, 133–141 (2015).

54. M. Raugei, S. Bargigli, S. Ulgiati, Life cycle assessment and energy pay-back time of advanced photovoltaic modules: CdTe and CIS compared to poly-Si. *Energy* **32**, 1310–1318 (2007).
55. A. Anctil, C. W. Babbitt, R. P. Raffaelle, B. J. Landi, Material and energy intensity of fullerene production. *Environ. Sci. Technol.* **45**, 2353–2359 (2011).
56. J. Zhang, X. Gao, Y. Deng, Y. Zha, C. Yuan, Comparison of life cycle environmental impacts of different perovskite solar cell systems. *Solar Energy Mater. Solar Cells* **166**, 9–17 (2017).
57. J.-A. Alberola-Borràs, R. Vidal, I. Mora-Seró, Evaluation of multiple cation/anion perovskite solar cells through life cycle assessment. *Sustainable Energy Fuels* **2**, 1600–1609 (2018).